1

X-Ray Spectroscopy Tools for the Characterization of Nanoparticles

Murid Hussain, Guido Saracco and Nunzio Russo
Politecnico di Torino
Italy

1. Introduction

Photocatalysts are solids that can promote reactions in the presence of light without being consumed in the overall reaction (Bhatkhande et al., 2001), and they are invariably semiconductors. A good photocatalyst should be photoactive, able to utilize visible and/or near UV light, biologically and chemically inert, photostable, inexpensive and non-toxic. For a semiconductor to be photochemically active as a sensitizer for the aforementioned reaction, the redox potential of the photogenerated valence band hole should be sufficiently positive to generate $OH^{\bullet}$ radicals that can subsequently oxidize the organic pollutant. The redox potential of the photogenerated conductance band electron must be sufficiently negative to be able to reduce the adsorbed O_2 to a superoxide. TiO_2, ZnO, WO_3, CdS, ZnS, $SrTiO_3$, SnO_2 and Fe_2O_3 can be used as photocatalysts.

TiO_2 is an ideal photocatalyst for several reasons (Bhatkhande et al., 2001; Fujishima et al., 2000, 2006; Mills & Hunte, 1997; Park et al., 1999; Peral et al., 1997; Periyat et al., 2008). It is relatively cheap, highly stable from a chemical point of view and easily available. Moreover, its photogenerated holes are highly oxidizing, and the photogenerated electrons are sufficiently reducing to produce superoxides from dioxygen groups. TiO_2 promotes ambient temperature oxidation of most indoor air pollutants and does not need any chemical additives. It has also been widely accepted and exploited as an efficient technology to kill bacteria.

Volatile organic compounds (VOCs) are considered to be as some of the most important anthropogenic pollutants generated in urban and industrial areas (Avila et al., 1998). VOCs are widely used in (and produced by) both industrial and domestic activities since they are ubiquitous chemicals that are used as industrial cleaning and degreasing solvents (Wang et al., 2007). VOCs come from many well-known indoor sources, including cooking and tobacco smoke, building materials, furnishings, dry cleaning agents, paints, glues, cosmetics, textiles, plastics, polishes, disinfectants, household insecticides, and combustion sources (Jo et al., 2004; Wang et al., 2007; Witte et al., 2008).

Moreover, ethylene (C_2H_4) is an odorless and colorless gas which exists in nature and is generated by human activities as a petrochemical derivative, from transport engine exhausts, and from thermal power plants (Saltveit, 1999). However, it is produced naturally by plant tissues and biomass fermentation and occurs along the food chain, in packages, in storage chambers, and in large commercial refrigerators (Martinez-Romero et al., 2007). The effect of ethylene on fruit ripening and vegetable senescence is of significant interest for the

scientific community. During the postharvest storage of fruit and vegetables, ethylene can induce negative effects, such as senescence, overripening, accelerated quality loss, increased fruit pathogen susceptibility, and physiological disorders. Fruit, vegetables, and flowers have ethylene receptors on their surface. Their actuation promotes ethylene production by the fruit itself and accelerates its ripening and aging (Kartheuser & Boonaert, 2007). Thus, the prevention of postharvest ethylene action is an important goal. Conventional as well as commercial techniques and technologies are used to control the action of ethylene, e. g. ethylene scavengers, especially the potassium permanganate ($KMnO_4$) oxidizer. However, $KMnO_4$ cannot be used in contact with food products due to its high toxicity. Ozone (O_3) is also an alternative oxidant, but it is highly unstable and decomposes into O_2 in a very short time. Carbons and zeolites are used as ethylene adsorbers and they play a key role in the control of ethylene. This technique only transfers the ethylene to another phase rather than destroying it. Hence, additional disposal or handling steps are needed.

New, safe and clean chemical technologies and processes for VOC and ethylene (generated by fruit) abatement are currently being developed (Hussain et al., 2010, 2011a, 2011b, Toma et al., 2006). Conventionally, VOC pollutants are removed by air purifiers that employ filters to remove particulate matter or use sorption materials (e.g. granular activated carbon) to adsorb the VOC molecules. These techniques also transfer the contaminants to another phase instead of destroying them and hence, additional disposal or handling steps are again needed. Moreover, all these sequestration techniques have inherent limitations, and none of them is decisively cost effective. Therefore, there is great demand for a more cost effective and environmentally friendly process that is capable of eliminating VOCs from gas streams, for example photochemical degradation, UV photolysis and photo-oxidation in the presence of some oxidants such as ozone. The photocatalytic oxidation (PCO) of VOCs is a very attractive and promising alternative technology for air purification. It has been demonstrated that organics can be oxidized to carbon dioxide, water and simple mineral acids at low temperatures on TiO_2 catalysts in the presence of UV or near-UV illumination. PCO requires a low temperature and pressure, employs inexpensive semiconducting catalysts, and is suitable for the oxidation of a wide range of organics. Some researchers (Augugliaro et al., 1999; Kumar et al., 2005) have already focused on this promising technique, and a great deal of beneficial advancement has been made in the field of VOC abatement. The performance of semiconducting photocatalyst depends above all on its nature and morphology.

Most of the studies have shown that the photocatalytic activity of titanium dioxide is influenced to a great extent by the crystalline form, although controversial results have also been reported in the literature. Some authors have stated that anatase works better than rutile (Zuo et al., 2006), others have found the best photocatalytic activity for rutile (Watson et al., 2003), and some others have detected synergistic effects in the photocatalytic activity for anatase–rutile mixed phases (Bacsa & Kiwi, 1998). It has recently been demonstrated that photo-activity towards organic degradation depends on the phase composition and on the oxidizing agent; for example, when the performance of different crystalline forms was compared, it was discovered that rutile shows the highest photocatalytic activity with H_2O_2, whereas anatase shows the highest with O_2 (Testino et al., 2007). It has also been found that photoformed OH species, as well as O^{2-} and O^{3-} anion radicals, play a significant role as a key active species in the complete photocatalytic oxidation of ethylene with oxygen into carbon dioxide and water (Kumar et al., 2005).

Therefore, in this chapter we have focused in particular on the synthesis of titania nanoparticles (TNP) at a large scale by controlling the optimized operating conditions and using a special passive mixer or vortex reactor (VR) to achieve TNPs with a high surface area and a mixed crystalline phase with more anatase and small amounts of rutile in order to obtain the synergistic effect that occurs between anatase and rutile. These TNPs were characterized and compared with TiO_2, synthesized by the solution combustion (TSC) method, and commercially available TiO_2 by Degussa P-25 and Aldrich. X-ray diffraction (XRD), energy dispersive X-ray (EDX) spectroscopy and X-ray photoelectron spectroscopy (XPS) techniques were used to screen the best candidate with the best characteristics for the above mentioned catalytic applications.

2. Titania synthesis and optimization by means of the XRD technique

Many processes can be employed to produce titanium dioxide particles, e. g. flame aerosol synthesis, hydrothermal synthesis, and sol–gel synthesis (Hussain et al., 2010). Flame aerosol synthesis offers the main advantage of being easily scalable to the industrial level, but also suffers from all the disadvantages of high temperature synthesis. Hydrothermal synthesis is instead particularly interesting as it directly produces a crystalline powder, without the need of a final calcination step, which is necessary in the sol–gel process. However, a lack of knowledge on the chemical equilibria of the species in solution and on the kinetics of the nucleation and growth of the different phases makes it difficult to control the overall process. Therefore, at the moment, the sol–gel process is the most common and promising at a lab scale. Although the sol–gel process has been known for almost a century and some of the most important aspects have been clarified, there is still room for improvement as far as individuating the synthesis conditions that result in a powder with improved properties, compared with the commercial products that are currently available, is concerned. Furthermore, upscaling the process from the laboratory to the industrial scale is still a complex and difficult to solve problem. Mixing plays an important role, but its effects are usually underestimated, as can be seen by the qualitative statements (e.g. add drop wise or mix vigorously) that are generally used to define ideal mixing conditions.

In our previous studies, TNPs were synthesized at a large scale (2 L gel), and the optimized operating parameters were controlled using the vortex reactor (VR) (Hussain et al., 2010, 2011a). Titanium tetra-isopropoxide (TTIP: Sigma–Aldrich) was used as a precursor in these studies, because of its very rapid hydrolysis kinetics. Two solutions of TTIP in isopropyl alcohol and of water (Milli-Q) in isopropyl alcohol were prepared separately under a nitrogen flux to control the alkoxide reactivity with humidity. Hydrochloric acid (HCl: Sigma–Aldrich) was added to the second solution as a hydrolysis catalyst and deagglomeration agent. The TTIP/isopropanol concentration was taken equal to 1 M to obtain the maximum TiO_2 (1 M), whereas the water and hydrochloric acid concentrations were chosen in order to result in a water-to-precursor ratio, $W= [H_2O]/[TTIP]$, equal to four, and an acid-to-precursor ratio, $H= [H^+]/[TTIP]$, equal to 0.5. The two TTIP and water solutions in isopropyl alcohol were stored in two identical vessels, then pressurized at 2 bars with analytical grade nitrogen, and eventually fed and mixed in the VR. The inlet flow rates were kept equal to 100 mL/min by using two rotameters. This inlet flow rate guarantees very fast mixing, and induces the formation of very fine particle. Equal volumes of reactant solutions (i.e. 1 L) were mixed at equal flow rates at 28 °C and then, for both configurations, the solutions exiting the VR were collected in a beaker thermostated at 28 °C and gently

stirred. The TTIP conversion into TiO_2 through hydrolysis and condensation can be summarized in the following overall chemical reaction:

$$Ti(OC_3H_7)_4 + 4H_2O \rightarrow TiO_2 + 2H_2O + 4C_3H_7OH$$

It is well known that a very fast chemical reaction is characterized by an equilibrium that is completely shifted towards the products, and that TiO_2 is a thermodynamically very stable substance which results in an almost 100% yield. The reaction product (i.e. gel) was dried in three different ways; dried by a rotavapor, directly in an oven, and in an oven after filtration. The resulting dried powders were eventually calcined at 400 °C for 3 h. TSC was synthesized by following the procedure reported in (Sivalingam et al., 2003), but with modified precursors and ratios. TTIP was used as the precursor, glycine/urea as the fuel, at stoichiometric as well as non-stoichiometric ratios, and 400/500 °C was adopted as the combustion temperature. After the combustion reaction, the samples were calcined at 400 °C for 3 h. Different commercial TiO_2 were purchased from Sigma–Aldrich and Aerosil for comparison purposes.

The TNPs were dried according to three different commercial processes in order to find the best method. After drying and before calcination, the powder is mainly amorphous and no distinct peak can be observed, as shown in Fig. 1 (Hussain et al., 2010). However, after calcination at 400 °C for 3 h, the main crystalline form was anatase (denoted as "A") and rutile (denoted as "R") was present to a lower extent (Fig. 1). The optimal drying condition was found by drying in a rotavapor, this resulted in an anatase-to-rutile ratio of 80:20. Details and a comparison with the other drying conditions are reported in Table 1. Compared to TNP, TSC showed a greater rutile phase in all the cases shown in Fig. 2. However, TSC (glycine, 500 °C, 1:1) and TSC (urea, 500 °C, 1:3) were comparatively better in this category, as shown in Table 1. Fig. 3 shows the XRD patterns of three different commercial TiO_2. The TiO_2 by Aldrich (anatase) showed a pure anatase phase whereas the TiO_2 by Aldrich (technical) had a mixed phase. Degussa P 25 also showed mixed anatase and rutile phases.

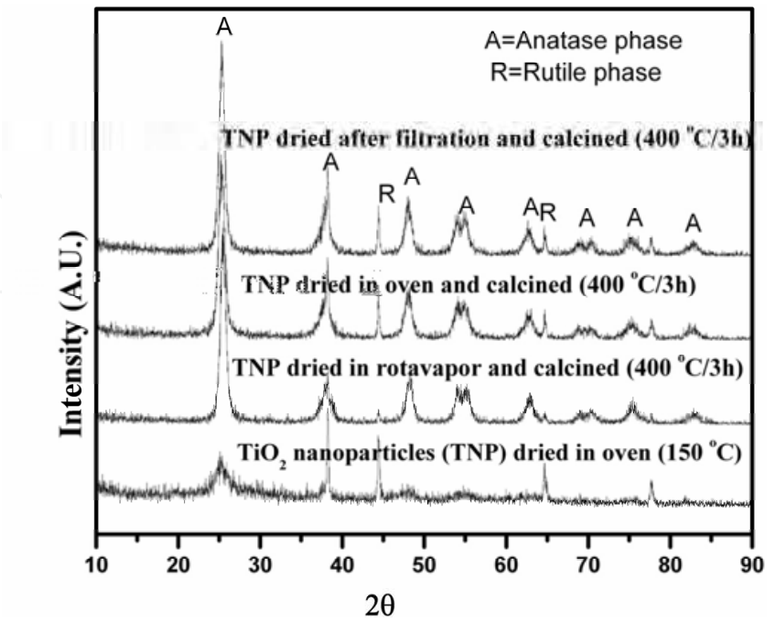

Fig. 1. XRD patterns of different dried TNPs showing the anatase and rutile phases

In order to determine the different polymorphs, XRD patterns were recorded on an X'Pert Phillips diffractomer using Cu Kα radiation, in the following conditions: range = (10–90°) 2θ; step size 2θ = 0.02. Moreover, quantification of the anatase:rutile phases was performed on the basis of the X'Pert database library (Hussain et al., 2010).

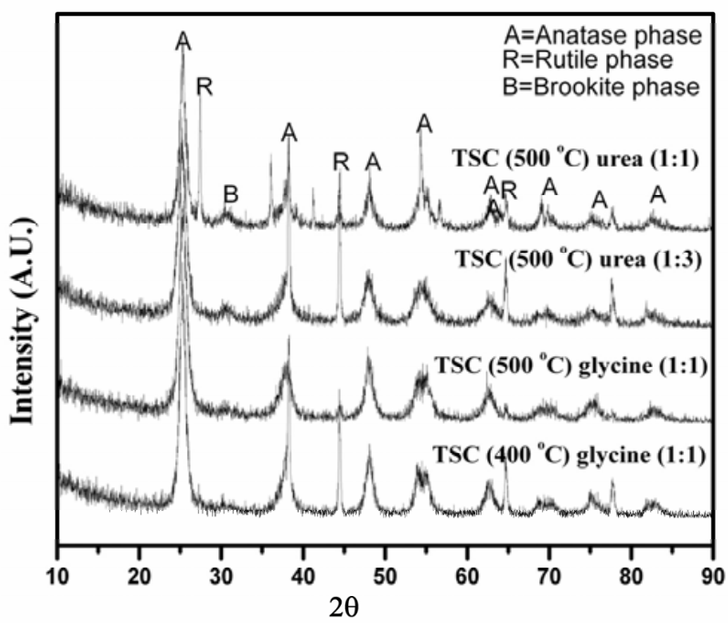

Fig. 2. XRD patterns of different titania synthesized by the solution combustion method (TSC) showing the anatase and rutile phases

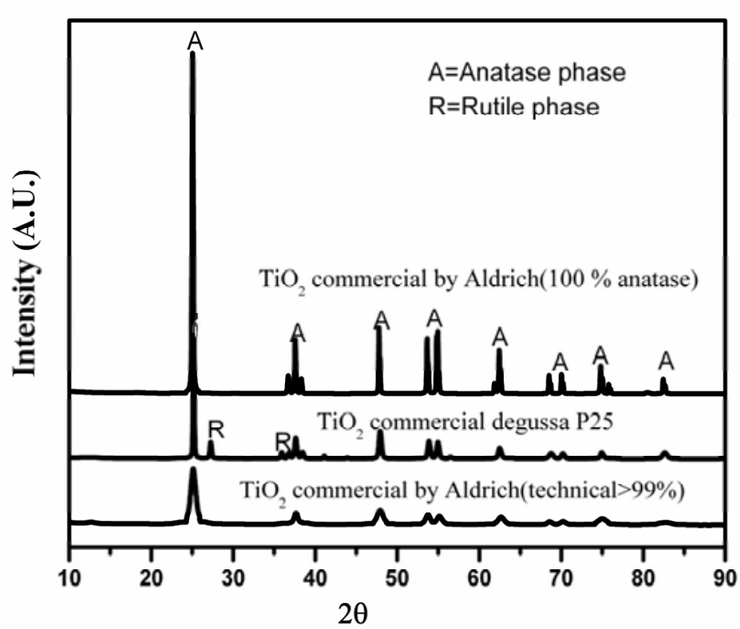

Fig. 3. XRD patterns of different commercial titania showing the anatase and rutile phases

Sample	Anatase:Rutile (%)
TNP (rotavapor dried and calcined)	80:20
TNP (filtered, dried and calcined)	71:29
TNP (oven dried and calcined)	69:31
TSC (glycine, 400 °C, 1:1)	55:45
TSC (glycine, 500 °C, 1:1)	60:40
TSC (urea, 500 °C, 1:3)	61:39
TSC (urea, 500 °C, 1:1)	58:42
TiO_2 commercial (aldrich, technical)	80:20
TiO_2 commercial (aldrich, anatase)	100:0
TiO_2 commercial (degussa P 25)	70:30

Table 1. Crystalline phases of different TiO_2 obtained by means of XRD

It is generally accepted that anatase demonstrates a higher activity than rutile, for most photocatalytic reaction systems, and this enhancement in photoactivity has been ascribed to the fact that the Fermi level of anatase is higher than that of rutile (Porkodi & Arokiamary, 2007). The precursors and the preparation method both affect the physicochemical properties of the specimen. In recent years, Degussa P 25 TiO_2 has set the standard for photoreactivity in environmental VOC applications. Degussa P 25 is a non-porous 70:30% (anatase to rutile) material. Despite the presence of the rutile phase, this material has proved to be even more reactive than pure anatase (Bhatkhande et al., 2001). Therefore, a mixed anatase–rutile phase seems to be preferable to enable some synergistic effects for photocatalytic reactions since the conduction band electron of the anatase partly jumps to the less positive rutile part, thus reducing the recombination rate of the electrons and the positive holes in the anatase part. The synthesized TNP is characterized by a similar anatase–rutile mixture.

Fig. 4(a) (Hussain et al., 2011a) shows the effect of calcination temperatures at a specific moderate calcination time (3 h) on the TNP by XRD patterns in order to establish the optimized calcination temperature. It was found that when the calcination temperature was below 500 °C, the TNP sample dominantly displayed the anatase phase with just small amounts of rutile. The synthesized TNP was dried in a rotary evaporator and this process was followed by complete water evaporation at 150 °C in an oven before calcination. Just after drying, the powder was mainly amorphous and no distinct peak was found, as shown in Fig. 4(b), although there were some very low intensity peaks at 2θ = 38.47, 44.7, 65.0 and 78.2, which were due to the aluminum sample holder. These aluminum sample holder peaks can also be observed in other samples, as shown in Fig. 4. The effect of calcination times on the characteristics of TNP is shown in Fig. 4(b); these data indicate that even the longer calcination time (7 h) has no significant effect on the TNP and the main phase remains anatase with low amounts of rutile. Therefore, the effect of calcination times at 400 °C is not so severe.

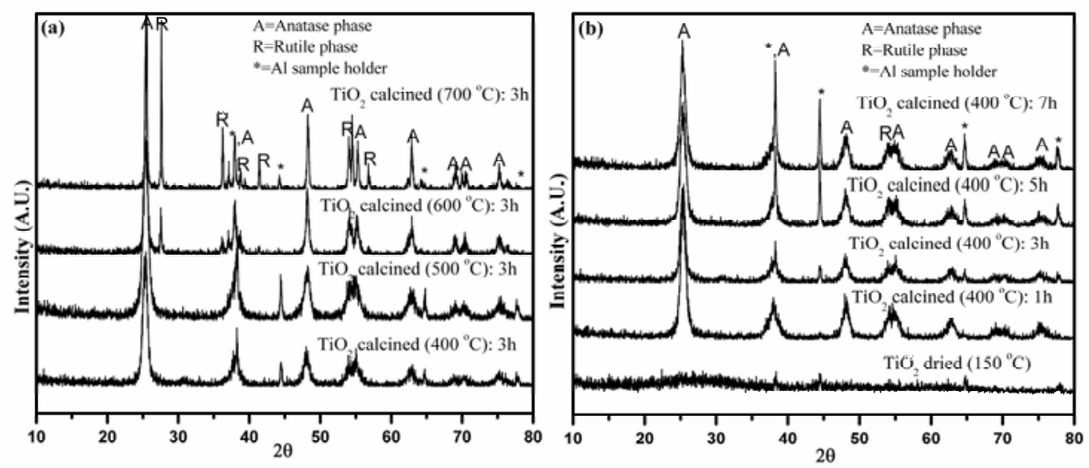

Fig. 4. XRD patterns of TNP at different calcinations (a) temperatures and (b) times

3. Synthesis confirmation of optimized TNP with EDX analysis

The elemental composition of TNPs was checked by EDX analysis equipping a high-resolution FE-SEM instrument (LEO 1525). Figure 5 shows the EDX analysis of the optimized TNP (dried by rotavapor and calcined at 400 °C for 3 h). This figure demonstrates that the main components are O and Ti with small amounts of Cl impurity. This Cl impurity originated from the HCl that was added during the synthesis and it is usually favorable for the photocatalytic reaction (Hussain et al., 2011b).

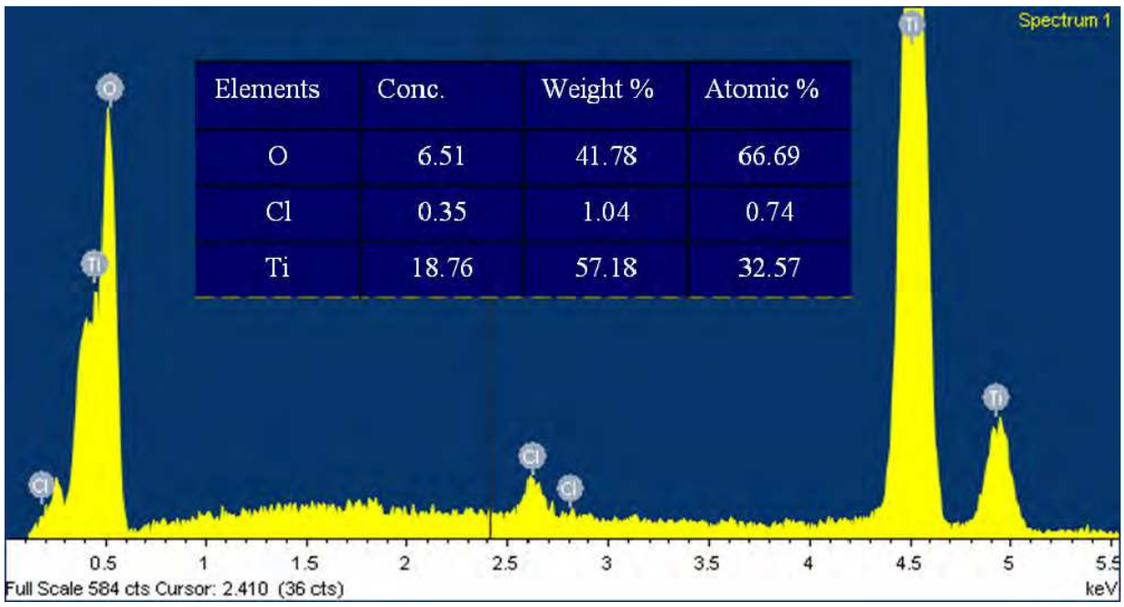

Fig. 5. EDX analysis of TNP

4. Photocatalytic reaction

All the ethylene, propylene, and toluene photocatalytic degradation tests were performed in a Pyrex glass reactor with a total volume of 2 L. The experimental setup of the photocatalysis reaction includes a Pyrex glass reactor (transparent to UV light), connectors, mass flow controllers (MFC, Bronkhorst high tech), and a UV lamp (Osram ULTRA-VITALUX 300W. This lamp has a mixture of UVA light ranging from 320–400 nm and UVB light with a 290–320 nm wavelength which produces 13.6 and 3.0 W radiations, respectively; it is ozone-free and the radiations are produced by a mixture of quartz burner and a tungsten wire filament, as mentioned in the manufacturer's indications). The set up also has gas cylinders (1000ppm ethylene/propylene/toluene), a gas chromatograph (Varian CP-3800) equipped with a capillary column (CP7381) and a flame ionization detector (FID) with a patented ceramic flame tip for ultimate peak shape and sensitivity, which was used for the gas analysis of the products (Hussain et al., 2010, 2011a, 2011b).

4.1 Screening of the best photocatalyst for ethylene photodegradation

The calcined TiO_2 photocatalyst sample was spread homogeneously, by hand, on a support placed inside the Pyrex glass reactor. An initial humidity of 60% was supplied to the photocatalyst to initiate the photocatalytic reaction. The VOC (ethylene, propylene or toluene) was continuously flushed in the reactor, with the help of the MFC, at a constant flow rate of 100 mL/min. After achieving equilibrium in the peak intensity, the UV light was turned on, the reaction products were analyzed by GC, and the conversion was calculated. The reaction experiments were repeated twice and the results showed reproducibility.

PCO of the ethylene over TNP was performed at ambient temperature and compared with different TSC and commercial TiO_2 photocatalysts. The important feature of this reaction is the use of air instead of conventional oxygen. In this situation, the required oxygen for the photocatalytic reaction is obtained from the air, leading towards the commercialization step. Fig. 6 shows the percentage conversion of ethylene as a function of time (Hussain et al., 2010). The TNP showed significantly higher conversion than all the other samples. Degussa P 25 showed comparable results. Even the 100% anatase commercial TiO_2 showed very low conversion in this reaction. Obviously, TSC synthesized in different ways using urea and glycine were also not suitable for this application. The TNP was active for 6 h of reaction time, unlike degussa P 25, which started to deactivate at this time. This deactivation of degussa P 25 is due to its inferior properties. Moreover, the TNP showed higher activity and better stability because of its superior properties. The main superior characteristic of TNP in ethylene photodegradation is that it has a main anatase phase with limited rutile (Table 1). The photocatalyst become active when photons of a certain wavelength hit the surface, which promotes electrons from the valence band and transfers them to the conductance band (Bhatkhande et al., 2001). This leaves positive holes in the valence band, and these react with the hydroxylated surface to produce $OH^{\bullet}$ radicals, which are the most active oxidizing agents. In the absence of suitable electron and hole scavengers, the stored energy is dissipated, within a few nanoseconds, by recombination. If a suitable scavenger or a surface defect state is available to trap the electron or hole, their recombination is prevented and a subsequent redox reaction may occur. In TNP, which is similar to degussa P 25, the conduction band electron of the anatase part jumps to the less positive rutile part, thus reducing the rate of recombination of the electrons and positive holes in the anatase part.

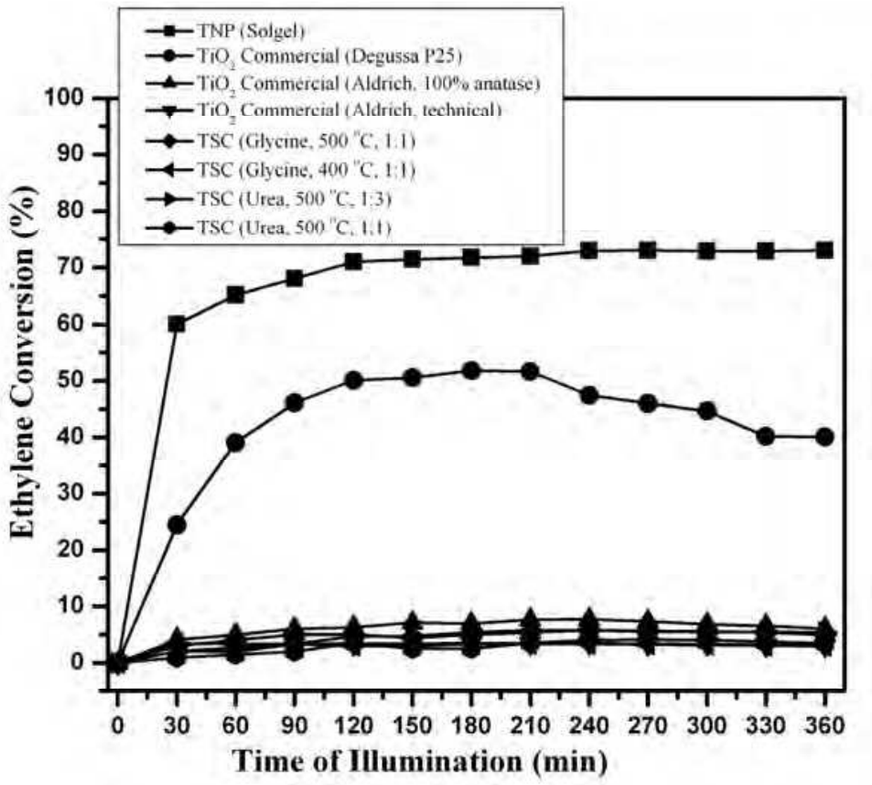

Fig. 6. Ethylene photodegradation over different titania photocatalysts with the illumination time

4.2 Optimization of photocatalyst for ethylene photodegradation

The PCO of ethylene was performed at ambient temperature over TNPs calcined at different calcination temperatures and times (Fig. 7) in order to check the catalytic performance of the developed TNP material (Hussain et al., 2011a). Air was again used instead of conventional oxygen in order to obtain more representative data for practical application conditions, in view of commercialization. After a preliminary saturation of the sample under an ethylene flow, conversion did not occur in the dark in any of the experiments, even in the presence of a catalyst or in the presence of UV light and the absence of a catalyst. Therefore, it can be concluded that the reaction results reported hereafter are only induced photocatalytically. Figs. 7(a) and 7(b) show the percentage conversion of ethylene as a function of illumination time. A steady-state conversion is reached after approximately 6 h of illumination for all the samples. This rather long time is necessary because of the type of experimental apparatus that has been employed; on the one hand because of fluid-dynamic reasons and on the other hand to make the surface of the sample reach a steady, equilibrium coverage value. The CO and CO_2 measurements of the outlet gases demonstrated that ethylene oxidizes completely to CO_2, and only traces of CO are observable. The TNP sample at the highest calcination temperature (700 °C) showed the worst performance, as can be observed in Fig. 7(a). However, the highest conversion was obtained for TNP calcined at 400 °C for 3 h. As expected, all the other sample preparation conditions resulted in a lower catalytic activity. In other words, the TNP sample at the highest calcination time (7 h), also showed the lowest

activity, as shown in Fig. 7(b). These reaction results of TNP calcined at different calcination temperatures and times are in perfect agreement with the characterization results of their XRD analysis. The TNP sample calcined at 400 °C for 3 h proved to be the best performing of all the samples. As previously mentioned, it possesses superior characteristics of the mixed anatase (80%)–rutile(20%) phase, a confined band gap energy of 3.17 eV, and the highest BET specific surface area, of 151 m^2/g, compared to all the others and therefore showed the best catalytic performance.

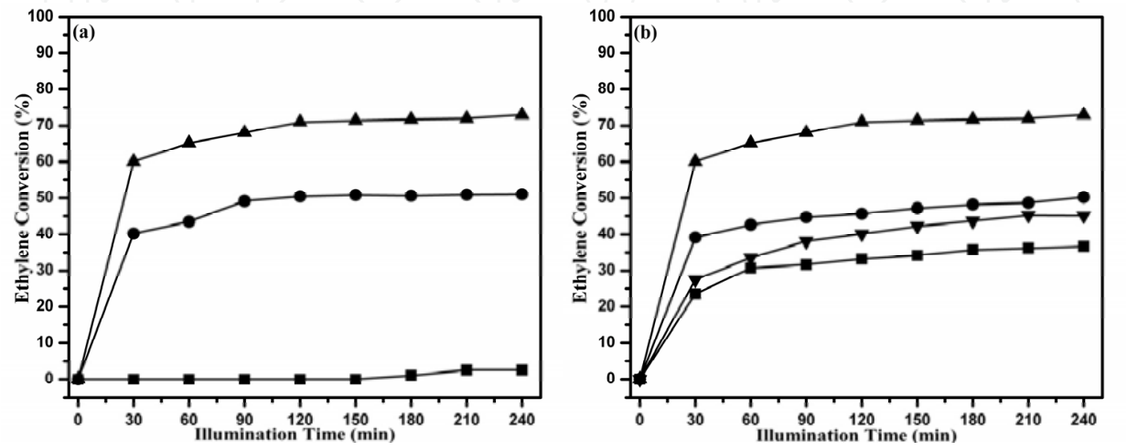

Fig. 7. Ethylene oxidation over TNP photocatalysts at different calcination (a) temperatures: (▲) 400 °C/3 h; (●) 600 °C/3 h; (■) 700 °C/3 h and (b) times: (▼) 400 °C/1 h; (▲) 400 °C/3 h; (●) 400 °C/5 h; (■) 400 °C/7 h. Operating conditions: feed concentration = 200 ppm; flow rate = 100 mL/min, room temperature; 1 g of TNP catalyst

4.3 Optimized TNP vs Degussa P 25 titania for VOC photodegradation

Fig. 8 shows a comparison of the optimized TNP and the Degussa P 25 catalysts for ethylene, propylene, and toluene at room temperature (Hussain et al., 2011a). In all three cases of VOC photodegradation for mineralization, the optimized TNP has shown a better activity and stability than that of Degussa P 25. TNP has small nanoparticles with a higher surface area and porosity than the non-porous Degussa P 25 (Hussain et al., 2010). It is also possible that the TNP material has a more amenable anataseto-rutile ratio (80:20) compared to Degussa P 25. Anatase phase based TiO_2 is usually better than rutile for photocatalytic reactions, due to its better adsorption affinity (Periyat et al., 2008). This difference is due to the structural difference of anatase and rutile. Both anatase and rutile have tetragonal structures with $[TiO_6]^{2-}$ octahedra, which share edges and corners in different ways, but maintain the overall TiO_2 stoichiometry. Four edges of the $[TiO_6]^{2-}$ octahedra are shared in anatase and a zigzag chain of octahedra that are linked to each other through shared edges is thus formed, but as far as rutile is concerned, two opposite edges of each $[TiO_6]^{2-}$ octahedra are shared to form the corner oxygen atoms. For this reason, the surface properties of anatase and rutile show considerable differences. Rutile is characterized by a surface on which the dissociation of the adsorbed organic molecules takes place much more easily than on anatase. These essential differences in the surface chemistry of the two TiO_2 phases result in differences in photocatalytic properties since the photocatalysis reactions mainly take place on the surface of the catalyst rather than in the bulk. Rutile titania has a

much lower specific surface area than that of anatase. As the specific surface area of the catalyst increases, it can adsorb more VOCs. Moreover, anatase exhibits lower electron–hole recombination rates than rutile due to its 10-fold greater electron trapping rate. Therefore, the mixed optimized TNP phase with a high surface area is the main characteristic which makes it better than Degussa P 25. The XRD data shown in Figs. 1-4 and Table 1 support this affirmation.

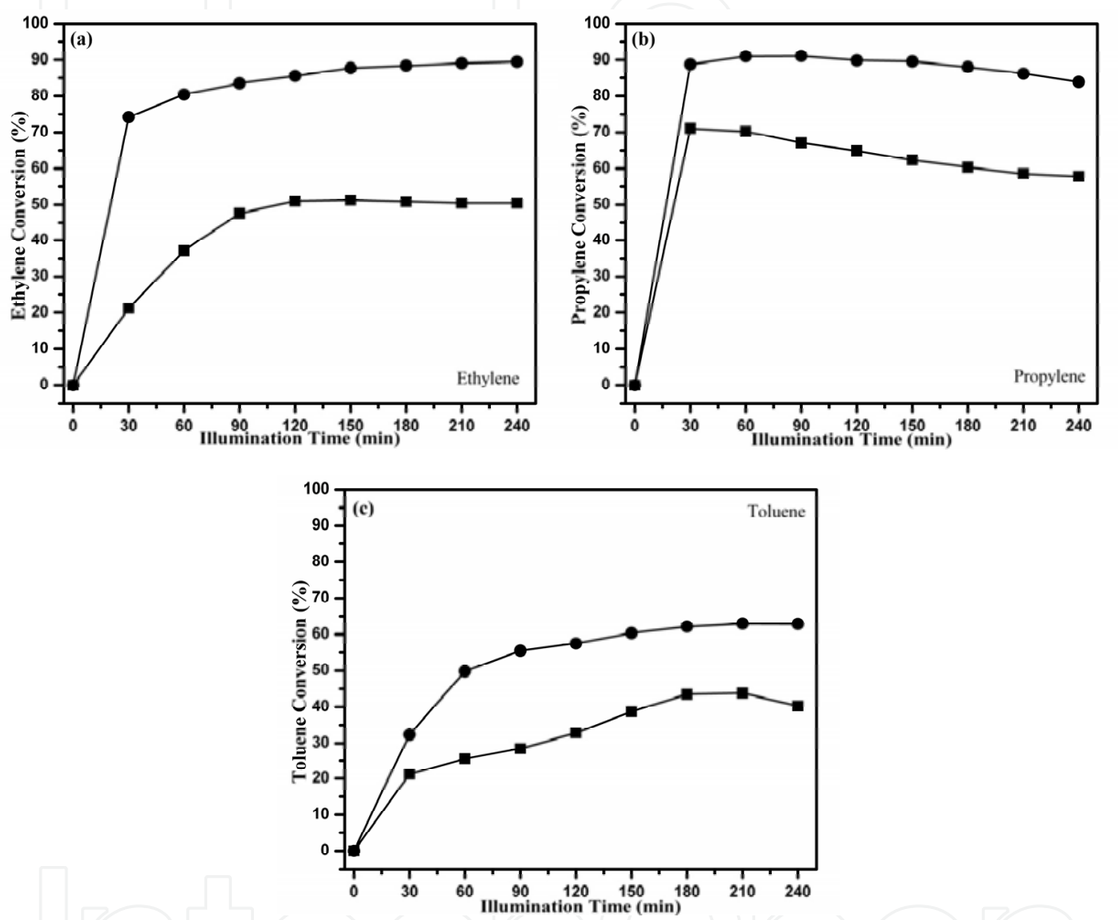

Fig. 8. Comparison of the optimized TNP vs. Degussa P 25 for VOC abatement (a) ethylene, (b) propylene, (c) toluene, fed at 100 ppm, in a 100 mL/min flow rate, over 1 g of catalyst at room temperature: (●) TNP (400 °C/3 h); (■) Degussa P 25

4.4 Optimized TNP vs Degussa P 25 titania for VOC photodegradation

The photocatalytic degradation of ethylene was performed in the reaction system explained in (Hussain et al., 2011b), at 3 °C, using ice, an artificial temperature atmosphere that is very similar to that commonly used for the cold storage of fruit. Air was also used here instead of conventional oxygen for the photocatalytic reaction to obtain more representative data of practical application conditions, for commercialization purposes.

Fig. 9(a) shows the effect of surface hydroxyl groups on ethylene degradation (Hussain et al., 2011b). The ethylene degradation reduced very significantly as the surface hydroxyl groups decreased due to increasing calcination temperature.

It has been observed that water has a significant effect on the photocatalytic degradation of ethylene, as shown in Fig. 9(b). After complete drying of the titania, the ethylene degradation reduced significantly. It became very low at the initial illumination time, due to a lack of water, which is necessary for the reaction. However, there was a slight improvement as illumination time increased, which might be due to the water produced during the reaction. This was confirmed when the fully dried titania was kept in a closed vessel with water for 12 h. After 12 h of contact time, the titania showed much higher activity than the fully dried samples. However, there was a slight improvement in ethylene degradation after keeping the normal titania in contact with water. In all of these cases, the TNPs showed better ethylene degradation than Degussa P 25, which might be due to the higher surface area of TNPs available for the adsorption of water and ethylene.

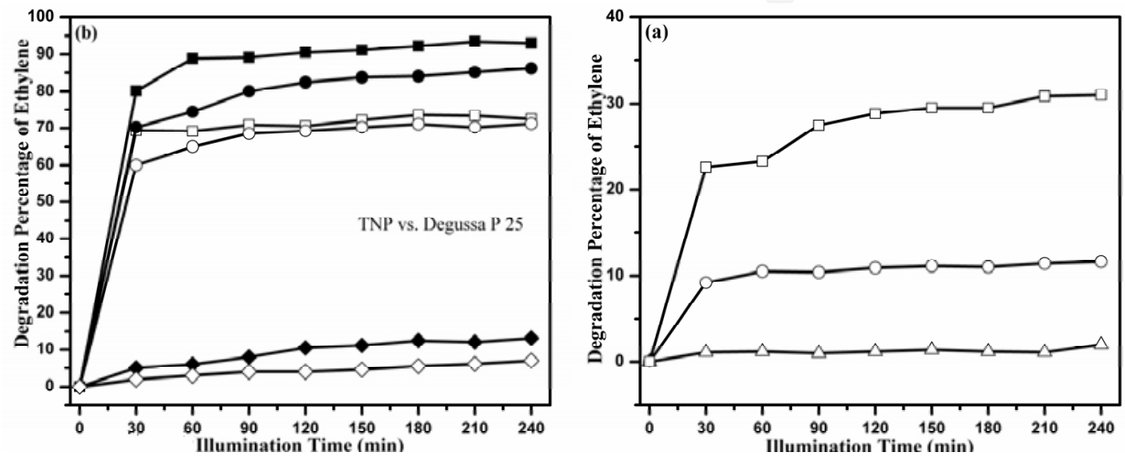

Fig. 9. (a) Effect of OH groups on ethylene degradation at 100 ppm, 100 mL/min flow rate, 3 °C using ice, and 1 g of photocatalyst: (□) TNP (400 °C/(3h))/UV lamp turned down to 75 cm; (○) TNP (600 °C/(3h))/UV lamp turned down to 75 cm; (Δ) TNP (800 °C/(3h))/UV lamp turned down to 75 cm, (b) Water effect on ethylene degradation over TNPs and Degussa P 25 photocatalysts at 100 ppm, 100 mL/min flow rate, 3 °C using ice, and 1 g of photocatalyst, UV lamp turned down to 12 cm/(short converging pipe + lens): (■) TNP kept with 1 g of water for 12 h before reaction; (□) Degussa P 25 kept with 1 g of water for 12 h before reaction; (●) TNP fully dried in oven at 150 °C for 12 h and then kept with water for 12 h before reaction; (○) Degussa P 25 fully dried in oven at 150 °C for 12 h and then kept with water for 12 h before reaction; (♦) TNP fully dried in oven at 150 °C for 12 h and immediate reaction; (◊) Degussa P 25 fully dried in oven at 150 °C for 12 h and immediate reaction.

5. XPS analysis of the optimized TNP vs Degussa P 25 titania

The XPS spectra were recorded using a PHI 5000 Versa Probe with a scanning ESCA microscope fitted with an Al monochromatic (1486.6 eV, 25.6 W) X-ray source, a beam diameter of 100 µm, a neutralizer at 1.4 eV and 20 mA, and a FAT analyzer mode. All the binding energies were referenced to the C1s peak at 284.6 eV of the surface carbon. The individual components were obtained by curve fitting (Hussain et al., 2011b).

XPS measurements were conducted to evaluate the hydroxyl groups and the evolution of the valence state of titanium on the TiO_2 surfaces. Fig. 10 shows the oxygen O1s XPS spectra

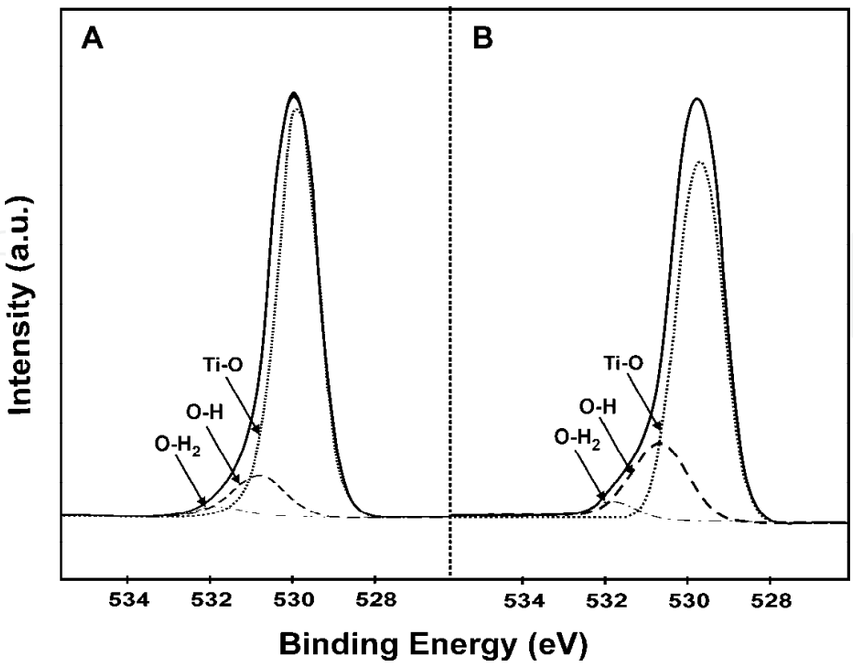

Fig. 10. XPS analysis showing the OH and O-H_2 comparison by O1s: (A) Degussa P 25; (B) TNPs

and the deconvolution results of the TNPs and Degussa P 25 from a quantitative point of view (Hussain et al., 2011b). The O1s spectrum displayed peaks at 529.6 eV associated with Ti-O bonds in TiO_2, at 530.8 eV, which correspond to the hydroxyl Ti-OH, (Hou et al., 2008; Kumar et al., 2000), whereas, at 532 eV, it shows Ti-OH_2 (Toma et al., 2006), which can be observed in the XPS spectra in Fig. 10 (A, Degussa P 25; B, TNPs). The TNPs clearly show more OH groups and OH_2 on the surface than Degussa P 25. The quantitative results are given in Table 1. The mass fraction of O1s, the hydroxyl groups, and the water of the two samples were calculated from the results of the curve fitting of the XPS spectra for the O1s region. The O1s values for the TNP and Degussa P 25 were 70.57 and 69.87%, respectively, and are similar. However, the O-H species for TNPs (22.59%) and Degussa P 25 (11.10%) are different. The water attached to Ti for TNPs (5.38%) and Degussa P 25 (2.29%) is also comparable. The higher OH groups on the surface of the TNPs than on Degussa P 25 might be responsible for obtaining superior photocatalytic activity in ethylene photodegradation at low temperature.

A comparison of the Ti2p spectra for TNPs and Degussa P 25 shows a $Ti2p_{3/2}$ peak at 458.5 and $Ti2p_{1/2}$ at 464 eV, as can be observed in Fig. 11(a) (Hussain et al., 2011b). The Ti species peaks, which occur at binding energies of 456.7 (Ti^{3+}) and 458.5 eV (Ti^{4+}) (Kumar et al., 2000), are shown in Fig. 11 for Degussa P 25 (B) and TNPs (C). It is clear that the TNPs have more Ti^{3+} species than Degussa P 25. After proper calculation through curve fitting, Table 2 shows that the TNP and Degussa P 25 catalysts have similar Ti2p values, but different Ti species. The TNP material has 17.77% Ti^{3+}, while Degussa P 25 only shows 8.93%. The Ti^{3+} species are responsible for oxygen photoadsorption, which results in the formation of O-ads, and which, together with the OH radical, is essential for photocatalytic oxidation (Fang et al., 2007; Suriye et al., 2007; Xu et al., 1999). The presence of surface Ti^{3+} causes distinct

differences in the nature of the chemical bonding between the adsorbed molecule and the substrate surface. These results are also correlated to the titania photocatalytic mechanism equations (1) and (2) (Hussain et al., 2011a) shown below:

$$Ti(IV) + e^{-} \rightarrow Ti(III) \quad (1)$$

$$Ti(III) + O_2 \rightarrow Ti(IV) + O_{2-} \quad (2)$$

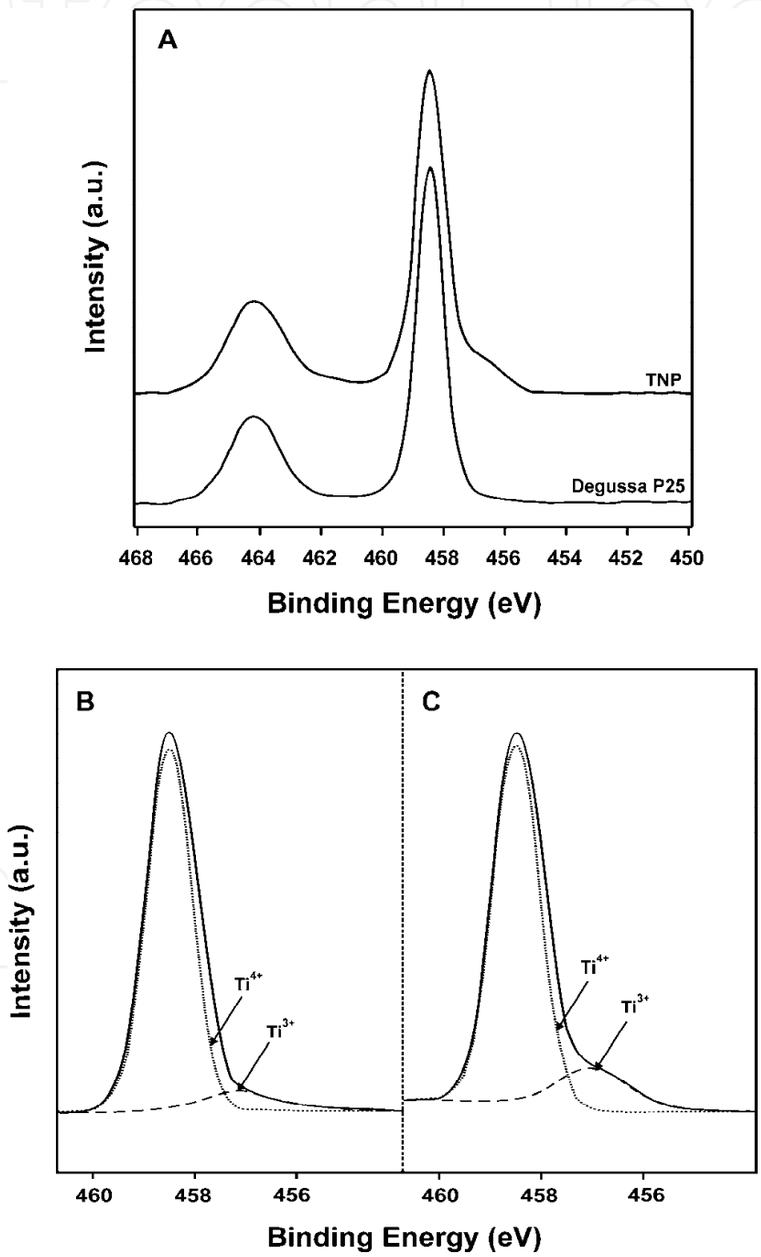

Fig. 11. XPS analysis showing the comparison between $Ti2p_{3/2}$ and $Ti2p_{1/2}$ (A), and the Ti species comparison: (B) Degussa P 25; (C) TNPs

Catalyst	O1s	$Ti2p_{3/2,1/2}$	Ti-O	O-H	$O\text{-}H_2$	Ti^{3+}	Ti^{4+}
Degussa P 25	69.87	30.13	86.61	11.10	2.29	8.93	91.07
TNP	70.57	29.43	72.03	22.59	5.38	17.77	82.23

Table 2. Atomic concentrations (%) of TiO_2 using XPS

6. Conclusion

An attempt has been made to synthesize titania nano-particles (TNP) at a large scale by controlling the optimized operating conditions and using a special passive mixer or vortex reactor (VR) to achieve TNPs with a high surface area and a mixed crystalline phase with more anatase and smaller amounts of rutile in order to obtain a synergistic effect between the anatase and rutile. These TNPs were characterized and compared with TiO_2 synthesized by means of the solution combustion (TSC) method and commercially available TiO_2 by Degussa P-25 and Aldrich. XRD and EDX spectroscopy techniques were used to establish the best candidate with the best characteristics for the above catalytic applications. A higher photocatalytic ethylene conversion was observed for TNP than for TSC or commercial TiO_2. The superior TNP photocatalyst was then further optimized by conducting an effective control of the calcination temperatures (400-700 ^oC) and times (1-7 h). The optimized TNP was achieved by calcining at 400 ^oC for 3 h, which also resulted in rather pure crystalline anatase with small traces of rutile, relatively more Ti^{3+} on the surface, and higher OH surface groups. This was confirmed by means of XRD and XPS investigations. The optimized TNP photocatalyst was then applied for photocatalytic degradation of different VOCs (ethylene, propylene and toluene) at near room temperature. Higher photocatalytic activity for VOC abatement was obtained for TNP than the Degussa P-25 TiO_2, due to the optimized mixed phase with a high surface area and the increased Ti^{3+} species, which might induce the adsorption of VOCs and water and generated OH groups which act as oxidizing agents on the TNP surface, leading to higher photocatalytic activity characteristics. The TNPs optimized with the help of XRD and XPS were also applied and compared with Degussa P-25 for the photocatalytic degradation of ethylene (emitted by fruit) at 3 ^oC to consider the possibility of its use for the cold storage of fruit. An efficient way of utilizing this optimized TNP photocatalyst for the target application has been developed. The role of the XRD, EDX and XPS characterization tools in the development of TNP for photocatalytic application seems to be very promising and encourages further research in this field.

7. Acknowledgment

M.H. is grateful to the Regione Piemonte and the Politecnico di Torino, Italy for his postdoctoral fellowship grant.

8. References

Augugliaro, V.; Coluccia, S.; Loddo, V.; Marchese, L.; Martra, G.; Palmisano, L. & Schiavello, M., (1999). Photocatalytic Oxidation of Gaseous Toluene on Anatase TiO_2 Catalyst: Mechanistic Aspects and FT-IR Investigation. *Appl. Catal. B: Environ.*, 20, 15–27, ISSN 0926-3373

Avila, P.; Bahamonde, A.; Blanco, J.; Sanchez, B.; Cardona, A. I. & Romero, M., (1998). Gas-Phase Photo-Assisted Mineralization of Volatile Organic Compounds by Monolithic Titania Catalysts. *Appl. Catal. B: Environ.,* 17, 75–88, ISSN 0926-3373

Bacsa, R. R. & Kiwi, J., (1998). Effect of Rutile Phase on the Photocatalytic Properties of Nanocrystalline Titania during the Degradation of p-Coumaric Acid. *Appl. Catal. B: Environ.,* 16, 19–29, ISSN 0926-3373

Bhatkhande, D. S.; Pangarkar, V. G. & Beenackers, A. A. C. M., (2001). Photocatalytic Degradation for Environmental Applications—a Review. *J. Chem. Technol. Biotechnol.,* 77, 102–116, ISSN 0268-2575

Fang, X.; Zhang, Z.; Chen, Q.; Ji, H. & Gao, X., (2007). Dependence of Nitrogen Doping on TiO_2 Precursor Annealed under NH_3 Flow. *J. Solid State Chem.*, 180, ISSN 1325-1332

Fujishima, A.; Rao, T. N. & Tryk, D. A., (2000). Titanium Dioxide Photocatalysis. *J. Photochem. Photobiol. C: Photochem. Rev.,* 1, 1–21, ISSN 1389-5567

Fujishima, A. & Zhang, X., (2006). Titanium Dioxide Photocatalysis: Present Situation and Future Approaches. *C. R. Chimie,* 9, 750–760, ISSN 1631-0748

Hou, Y. D.; Wang, X. C.; Wu, L.; Chen, Z. X.; Ding, X. X. & Fu, X. Z., (2008). N-Doped SiO_2/TiO_2 Mesoporous Nanoparticles with Enhanced Photocatalytic Activity under Visible-Light Irradiation. *Chemosphere,* 72, 414-421, ISSN 0045-6535

Hussain, M.; Ceccarelli, R., Marchisio, D. L.; Fino, D.; Russo, N. & Geobaldo, F., (2010). Synthesis, Characterization, and Photocatalytic Application of Novel TiO_2 Nanoparticles. *Chem. Eng. J.,* 157, 45–51, ISSN 1385-8947

Hussain, M.; Russo, N. & Saracco, G., (2011a). Photocatalytic Abatement of VOCs by Novel Optimized TiO_2 Nanoparticles. *Chem. Eng. J.,* 166, 138–149, ISSN 1385-8947

Hussain, M.; Bensaid, S.; Geobaldo, F.; Saracco, G. & Russo, N., (2011b). Photocatalytic Degradation of Ethylene Emitted by Fruits with TiO_2 Nanoparticles. *Ind. Eng. Chem. Res.*, 50, 2536-2543, ISSN 0888-5885

Jo, W.-K. & Park, K.-H., (2004). Heterogeneous Photocatalysis of Aromatic and Chlorinated Volatile Organic Compounds (VOCs) for Non-Occupational Indoor Air Application. *Chemosphere,* 57, 555–565, ISSN 0045-6535

Kartheuser, B. & Boonaert, C., (2007). Photocatalysis: A Powerful Technology for Cold Storage Applications. *J. Adv. Oxid. Technol.,* 10, 107-110, ISSN 1203-8407

Kumar, P. M.; Badrinarayanan, S. & Sastry, M., (2000). Nanocrystalline TiO_2 Studied by Optical, FT-IR and X-ray Photoelectron Spectroscopy: Correlation to Presence of Surface States. *Thin Solid Films,* 358, 122-130, ISSN 0040-6090

Kumar, S.; Fedorov, A. G. & Gole, J. L., (2005). Photodegradation of Ethylene using Visible Light Responsive Surfaces Prepared from Titania Nanoparticle Slurries. *Appl. Catal. B: Environ.,* 57, 93–107, ISSN 0926-3373

Martinez-Romero, D.; Bailen, G.; Serrano, M.; Guillen, F.; Valverde, J. M.; Zapata, P.; Castillo, S. & Valero, D., (2007). Tools to Maintain Postharvest Fruit and Vegetable Quality through the Inhibition of Ethylene Action: A Review. *Crit. Rev. Food Sci.,* 47, 543-560, ISSN 1040-8398

Mills, A. & Hunte, S. L., (1997). An Overview of Semiconductor Photocatalysis. *J. Photochem. Photobiol. A: Chem.,* 108, 1–35, ISSN 1010-6030

Park, D. R.; Zhang, J.; Ikeue, K.; Yamashita, H. & Anpo, M., (1999). Photocatalytic Oxidation of Ethylene to CO_2 and H_2O on Ultrafine Powdered TiO_2 Photocatalysts in the Presence of O_2 and H_2O. *J. Catal.,* 185, 114–119, ISSN 0021-9517

Peral, J.; Domenech, X. & Ollis, D. F., (1997). Heterogeneous Photocatalysis for Purification, Decontamination and Deodorization of Air. *J. Chem. Technol. Biotechnol.,* 70, 117–140, ISSN 0268-2575

Periyat, P.; Baiju, K. V.; Mukundan, P.; Pillai, P. K. & Warrier, K. G. K., (2008). High Temperature Stable Mesoporous Anatase TiO_2 Photocatalyst Achieved by Silica Addition. *Appl. Catal. A: Gen.,* 349, 13–19, ISSN 0926-860X

Porkodi, K. & Arokiamary, S. D., (2007). Synthesis and Spectroscopic Characterization of Nanostructured Anatase Titania: a Photocatalyst. *Mater. Charact.,* 58, 495–503, ISSN 1044-5803

Saltveit, M. E., (1999). Effect of Ethylene on Quality of Fresh Fruits and Vegetables. *Postharvest Biol. Technol.,* 15, 279-292, ISSN 0925-5214

Sivalingam, G.; Nagaveni, K.; Hegde, M. S. & Madras, G., (2003). Photocatalytic Degradation of Various Dyes by Combustion Synthesized Nano Anatase TiO_2. *Appl. Catal. B: Environ.,* 45, 23–38, ISSN 0926-3373

Suriye, K.; Praserthdam, P. & Jongsomjit, B., (2007). Control of Ti^{3+} Surface Defect on TiO_2 Nanocrystal using Various Calcination Atmospheres as the First Step for Surface Defect Creation and Its Application in Photocatalysis. Appl. Surf. Sci., 253, 3849-3855, ISSN 0169-4332

Testino, A.; Bellobono, I. R.; Buscaglia, V.; Canevali, C.; D'Arienzo, M.; Polizzi, S.; Scotti, R. & Morazzoni, F., (2007). Optimizing the Photocatalytic Properties of Hydrothermal TiO_2 by the Control of Phase Composition and Particle Morphology. A systematic Approach. *J. Am. Chem. Soc.,* 129, 3564–3575, ISSN 0002-7863

Toma, F.-L.; Bertrand, G.; Begin, S.; Meunier, C.; Barres, O.; Klein, D. & Coddet, C., (2006) Microstructure and Environmental Functionalities of TiO_2-Supported Photocatalysts Obtained by Suspension Plasma Spraying. *Appl. Catal., B: Environ.,* 68, 74-84, ISSN 0926-3373

Wang, S.; Ang, H. M. & Tade, M. O., (2007). Volatile Organic Compounds in Indoor Environment and Photocatalytic Oxidation: State of the Art. *Environ. Int.,* 33, 694–705, ISSN 0160-4120

Watson, S. S.; Beydoun, D.; Scott, J. A. & Amal, R., (2003). The Effect of Preparation Method on the Photoactivity of Crystalline Titanium Dioxide Particles. *Chem. Eng. J.,* 95, 213–220, ISSN 1385-8947

Witte, K. De; Meynen, V.; Mertens, M.; Lebedev, O. I.; Tendeloo, G. Van; Sepulveda-Escribano, A.; Rodriguez-Reinoso, F.; Vansant, E. F. & Cool, P., (2008). Multi-step Loading of Titania on Mesoporous Silica: Influence of the Morphology and the Porosity on the Catalytic Degradation of Aqueous Pollutants and VOCs. *Appl. Catal. B: Environ.,* 84, 125–132, ISSN 0926-3373

Xu, Z.; Shang, J.; Liu, C.; Kang, C.; Guo, H. & Du, Y., (1999). The Preparation and Characterization of TiO_2 Ultrafine Particles. *Mater. Sci. Eng. B,* 56, 211-214, ISSN 0921-5107

Zuo, G.-M.; Cheng, Z.-X.; Chen, H.; Li, G.-W. & Miao, T., (2006). Study on Photocatalytic Degradation of Several Volatile Organic Compounds. *J. Hazard. Mater.,* B 128, 158–163, ISSN 0304-3894

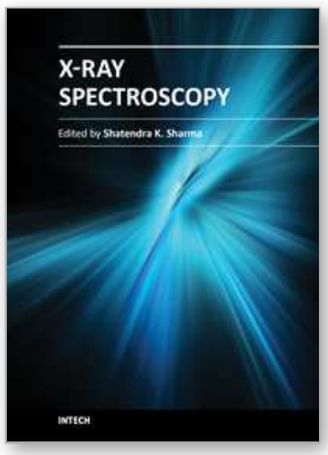

X-Ray Spectroscopy

Edited by Dr. Shatendra K Sharma

ISBN 978-953-307-967-7
Hard cover, 280 pages
Publisher InTech
Published online 01, February, 2012
Published in print edition February, 2012

The x-ray is the only invention that became a regular diagnostic tool in hospitals within a week of its first observation by Roentgen in 1895. Even today, x-rays are a great characterization tool at the hands of scientists working in almost every field, such as medicine, physics, material science, space science, chemistry, archeology, and metallurgy. With vast existing applications of x-rays, it is even more surprising that every day people are finding new applications of x-rays or refining the existing techniques. This book consists of selected chapters on the recent applications of x-ray spectroscopy that are of great interest to the scientists and engineers working in the fields of material science, physics, chemistry, astrophysics, astrochemistry, instrumentation, and techniques of x-ray based characterization. The chapters have been grouped into two major sections based upon the techniques and applications. The book covers some basic principles of satellite x-rays as characterization tools for chemical properties and the physics of detectors and x-ray spectrometer. The techniques like EDXRF, WDXRF, EPMA, satellites, micro-beam analysis, particle induced XRF, and matrix effects are discussed. The characterization of thin films and ceramic materials using x-rays is also covered.

How to reference

In order to correctly reference this scholarly work, feel free to copy and paste the following:

Murid Hussain, Guido Saracco and Nunzio Russo (2012). X-Ray Spectroscopy Tools for the Characterization of Nanoparticles, X-Ray Spectroscopy, Dr. Shatendra K Sharma (Ed.), ISBN: 978-953-307-967-7, InTech, Available from: http://www.intechopen.com/books/x-ray-spectroscopy/x-ray-spectroscopy-tools-for-the-characterization-of-nanoparticles

INTECH
open science | open minds

InTech Europe
University Campus STeP Ri
Slavka Krautzeka 83/A
51000 Rijeka, Croatia
Phone: +385 (51) 770 447
Fax: +385 (51) 686 166
www.intechopen.com

InTech China
Unit 405, Office Block, Hotel Equatorial Shanghai
No.65, Yan An Road (West), Shanghai, 200040, China
中国上海市延安西路65号上海国际贵都大饭店办公楼405单元
Phone: +86-21-62489820
Fax: +86-21-62489821

IntechOpen